A Letters Journal Exploring
the Frontiers of Physics

OFFPRINT

Spin and charge shot noise in mesoscopic spin Hall systems

R. L. Dragomirova, L. P. Zârbo and B. K. Nikolić

EPL, **84** (2008) 37004

A Letters Journal Exploring
the Frontiers of Physics

November 2008

EPL, **84** (2008) 37004
doi: 10.1209/0295-5075/84/37004

www.epljournal.org

Spin and charge shot noise in mesoscopic spin Hall systems

R. L. Dragomirova, L. P. Zârbo[(a)] and B. K. Nikolić

Department of Physics and Astronomy, University of Delaware - Newark, DE 19716-2570, USA

received 30 June 2008; accepted in final form 22 September 2008
published online 21 October 2008

PACS 72.25.Dc – Spin polarized transport in semiconductors
PACS 05.40.Ca – Noise

Abstract – Injection of unpolarized charge current through the longitudinal leads of a four-terminal two-dimensional electron gas with the Rashba spin-orbit (SO) coupling and SO scattering off extrinsic impurities is responsible not only for the pure spin Hall current in the transverse leads, but also for non-equilibrium random time-dependent current fluctuations. We employ the scattering approach to current-current correlations in multiterminal nanoscale conductors to analyze the shot noise of transverse pure spin Hall current and zero charge current, or transverse spin current and non-zero charge Hall current, driven by unpolarized or spin-polarized injected longitudinal charge current, respectively. Since any spin-flip acts as an additional source of noise, we argue that these shot noises provide a unique experimental tool to differentiate between intrinsic and extrinsic SO mechanisms underlying the spin Hall effect in paramagnetic devices.

Introduction. – The recently discovered spin Hall effect (SHE) in paramagnetic semiconductor [1,2] and metallic [3] systems holds great promise to revolutionize electrical generation, control, and detection of non-equilibrium spin populations in the envisioned "second generation" of spintronic devices [4]. The SHE actually denotes a *collection* of phenomena manifesting as transverse (with respect to injected longitudinal unpolarized charge current) separation of spin-↑ and spin-↓ states, which then comprise either a pure spin current or accumulate at the lateral sample boundaries. Its Onsager reciprocal phenomenon —the inverse SHE [5,6] where longitudinal pure spin current generates transverse charge current or voltage between the lateral boundaries— offers one of the most efficient schemes to detect elusive *pure* (not accompanied by any net charge flux) spin currents [7] by converting them into electrical quantities [3].

While SHE does not require external magnetic field, it essentially relies on the SO coupling effects in solids. In addition, its magnitude can depend on the type of microscopic SO interaction, impurities, charge density, geometry, and dimensionality. Such a variety of SHE manifestations poses immense challenge for attempts at a unified theoretical description of spin transport in the presence of relativistic effects, which has not been resolved by early hopes [7–9] that auxiliary spin current operator $\hat{j}_y^z$ and spin conductivity $\sigma_{sH} = \langle \hat{j}_y^z \rangle / E_x$ (as the linear response to longitudinal electric field E_x) of infinite homogeneous systems could be elevated to universally applicable and experimentally relevant quantities.

Thus, the key task emerging for theoretical analysis is to provide guidance for increasing and controlling the spin accumulation in confined geometries [10–12] (observed SHE in semiconductors is presently rather small [1,2]) or outflowing spin currents [10,13] driven by them. In this respect, understanding of the *intrinsic* [8,9,14] (due to SO-induced spin-split band structure) or *extrinsic* [5,15] (due to SO-dependent scattering off impurities) origin of the SHE has been one of the central topics in interpreting experiments [14] and development of SHE-based spintronic devices [4]. For example, the intrinsic SO couplings are predicted to yield much larger SHE response [14], which, moreover, can be controlled electrically by the gate electrodes covering low-dimensional devices [13,16]. The extrinsic ones are fixed and the corresponding much smaller SHE is hardly controllable (except through charge density and mobility [4]).

However, measurement of standard quantities associated with transverse spin and charge transport is often unable to resolve the intrinsic *vs.* extrinsic controversy [7,14] or probe the crossover between these limiting regimes [15]. This long-standing issue is well known from the studies of the anomalous Hall effect (AHE) [17] in ferromagnetic materials (SHE can be viewed as the zero magnetization limit of AHE). For example, the frequent

(a) Present address: Department of Physics, Texas A&M University - College Station, TX 77843-4242, USA.

analysis of the AHE experimental data —fitting of the Hall resistivity *vs.* longitudinal zero-field resistivity by a power law— is typically insufficient [18] to clearly differentiate a variety of mechanisms [15,17] driven by SO coupling effects.

Here lessons from mesoscopic quantum physics might shed new light: much more information about transport of non-interacting or interacting quasiparticles is contained in time-dependent non-equilibrium current (or voltage) fluctuations [19] than in traditional (time-averaged) conductances and conductivities. Unlike equilibrium (*i.e.*, thermally driven) noise, such *shot noise* persists down to zero temperature and it is fundamentally connected to the discrete nature of the electron charge [19]. Furthermore, a handful of recent theoretical [20–22] and experimental [23] studies have suggested that shot noise in systems with spin-dependent interactions provides a sensitive probe to differentiate between magnetic impurities, spin-flip scattering, and continuous spin precession effects on semiclassical or quantum transport of injected spin-polarized currents. This is due to the fact that any spin-flip converts a spin-↑ subsystem particle into a spin-↓ subsystem particle, where the two subsystems differ when spin degeneracy is lifted. Thus, the non-conservation of the number of particles in each subsystem generates additional source of current fluctuations.

In this letter we investigate whether the information stored in the shot noise of transverse spin Hall current, as well as the noise of associated transverse charge transport, can be used to separate different types of SO interactions driving the SHE. We draw inspiration for this approach from the following recent intriguing theoretical findings: i) the intrinsic aspects of AHE have been related to the transverse voltage shot noise [24] or longitudinally injected spin-polarized current noise [21] in ferromagnetic devices; ii) measurement of charge currents and their auto- and cross-correlation shot noise on a multiterminal bridge could be used to obtain the SHE conductance in terms of these *purely electrical* quantities (independently of the underlying microscopic SO mechanism) [25]; iii) shot noise of spin-polarized charge current offers a sensitive *all-electrical* probe of spin precession and spin dephasing in two-terminal nanostructures [22]. Our principal findings, summarized in figs. 1 and 2, suggest that in multiterminal two-dimensional electron gas (2DEG), whose SHE generally contains contributions from both the extrinsic and intrinsic SO couplings [26], the shot noise of spin and charge current in the transverse electrodes is substantially affected by the presence and magnitude of the intrinsic Rashba SO coupling. On the other hand, extrinsic SO coupling effects have virtually no effect on the shot noise in the transverse electrodes.

Scattering approach to shot noise of spin and charge currents in multiterminal nanostructures. – Unlike seminal arguments [9] for the intrinsic SHE in infinite 2DEGs, where the electric-field–driven acceleration of electron momenta and associated precession of spins [15] plays a crucial role, the so-called *mesoscopic* SHE [7,13] was introduced in ballistic finite-size systems attached to multiple current and voltage probes where electric field is absent in the SO-coupled central sample [13,27–29]. Its description [13] in terms of the total charge currents $I_\alpha = I_\alpha^\uparrow + I_\alpha^\downarrow$ and conserved total spin currents $I_\alpha^{S_z} = I_\alpha^\uparrow - I_\alpha^\downarrow$ (which are related to non-equilibrium spin densities within the sample [10]) outflowing through ideal (*i.e.*, spin and charge interaction-free) electrodes α is particularly suited for the spin-dependent multiterminal shot noise analysis.

To proceed with such analysis, we define correlators between spin-resolved charge currents $I_\alpha^\uparrow$ and $I_\beta^\downarrow$ in the same $\alpha = \beta$ or different $\alpha \neq \beta$ leads

$$S_{\alpha\beta}^{\sigma\sigma'}(t-t') = \frac{1}{2}\langle \delta\hat{I}_\alpha^\sigma(t)\delta\hat{I}_\beta^{\sigma'}(t') + \delta\hat{I}_\beta^{\sigma'}(t')\delta\hat{I}_\alpha^\sigma(t)\rangle. \quad (1)$$

Here $\hat{I}_\alpha^\sigma(t)$ is the quantum-mechanical operator of spin-resolved charge current of spin-σ ($\sigma = \uparrow, \downarrow$) electrons in lead α. The current-fluctuation operator at time t in lead α is given by

$$\delta\hat{I}_\alpha^\sigma(t) = \hat{I}_\alpha^\sigma(t) - \langle \hat{I}_\alpha^\sigma(t)\rangle. \quad (2)$$

We use $\langle \ldots \rangle$ to denote both quantum-mechanical and statistical averaging over the states in the macroscopic reservoirs to which a mesoscopic conductor is attached via semi-infinite leads [19]. The spin-resolved noise power between terminals α and β is the Fourier transform of eq. (1)

$$S_{\alpha\beta}^{\sigma\sigma'}(\omega) = 2\int \mathrm{d}(t-t')\, e^{-i\omega(t-t')} S_{\alpha\beta}^{\sigma\sigma'}(t-t'). \quad (3)$$

This gives

$$S_{\alpha\beta}^{\mathrm{charge}}(\omega) = S_{\alpha\beta}^{\uparrow\uparrow}(\omega) + S_{\alpha\beta}^{\downarrow\downarrow}(\omega) + S_{\alpha\beta}^{\uparrow\downarrow}(\omega) + S_{\alpha\beta}^{\downarrow\uparrow}(\omega), \quad (4)$$

for the charge current noise and

$$S_{\alpha\beta}^{\mathrm{spin}}(\omega) = S_{\alpha\beta}^{\uparrow\uparrow}(\omega) + S_{\alpha\beta}^{\downarrow\downarrow}(\omega) - S_{\alpha\beta}^{\uparrow\downarrow}(\omega) - S_{\alpha\beta}^{\downarrow\uparrow}(\omega), \quad (5)$$

for the spin current noise.

In the scattering theory of quantum transport, the operator of spin-resolved charge current carrying spin-σ electrons through terminal α is expressed as

$$\hat{I}_\alpha^\sigma(t) = \frac{e}{h}\sum_{n=1}^{M}\iint \mathrm{d}E\,\mathrm{d}E'\, e^{i(E-E')t/\hbar}[\hat{a}_{\alpha n}^{\sigma\dagger}(E)\hat{a}_{\alpha n}^{\sigma}(E') - \hat{b}_{\alpha n}^{\sigma\dagger}(E)\hat{b}_{\alpha n}^{\sigma}(E')], \quad (6)$$

where the operators $\hat{a}_{\alpha n}^{\sigma\dagger}(E)$ ($\hat{a}_{\alpha n}^{\sigma}(E)$) create (annihilate) incoming electrons in lead α having energy E, spin-σ, and the orbital wave function (*i.e.*, "conducting channel") $|n\rangle$. The corresponding operators $\hat{b}_{\alpha n}^{\sigma\dagger}$, $\hat{b}_{\alpha n}^{\sigma}$ act on the outgoing states. Inserting $\hat{I}_\alpha^\sigma(t)$ into eq. (1) and Fourier transforming it leads to the following formula for the spin-resolved noise power spectrum:

$$S_{\alpha\beta}^{\sigma\sigma'}(\omega) = \frac{e^2}{h}\int \mathrm{d}E \sum_{\gamma,\gamma'}\sum_{\rho,\rho'=\uparrow,\downarrow} \mathrm{Tr}\left[\mathbf{A}_{\gamma\gamma'}^{\rho\rho'}(\alpha,\sigma,E,E+\hbar\omega) \times \mathbf{A}_{\gamma'\gamma}^{\rho'\rho}(\beta,\sigma',E+\hbar\omega,E)\right]\left\{f_\gamma^\rho(E)\left[1-f_{\gamma'}^{\rho'}(E+\hbar\omega)\right] + f_{\gamma'}^{\rho'}(E+\hbar\omega)[1-f_\gamma^\rho(E)]\right\}. \quad (7)$$

Here $f_\gamma^\rho(E)$ is the Fermi function of spin-ρ electrons ($\rho=\uparrow,\downarrow$), kept at temperature T and spin-dependent chemical potential μ_γ^ρ in lead γ. The Büttiker's current matrix [19] $\mathbf{A}_{\beta\gamma}^{\rho\rho'}(\alpha,\sigma,E,E')$, whose elements are $[\mathbf{A}_{\beta\gamma}^{\rho\rho'}(\alpha,\sigma,E,E')]_{mn}=\delta_{mn}\delta_{\beta\alpha}\delta_{\gamma\alpha}\delta^{\sigma\rho}\delta^{\sigma\rho'}-\sum_k[\mathbf{s}_{\alpha\beta}^{\sigma\rho\dagger}(E)]_{mk}[\mathbf{s}_{\alpha\gamma}^{\sigma\rho'}(E')]_{kn}$, is now generalized to include explicitly spin degrees of freedom through the spin-resolved scattering matrix connecting operators $\hat{a}_{\alpha n}^\sigma(E)$ and $\hat{b}_{\alpha n}^\sigma(E)$ via $\hat{b}_{\alpha n}^\sigma(E)=\sum_{\beta m}[\mathbf{s}_{\alpha\beta}^{\sigma\sigma'}]_{nm}(E)\hat{a}_{\beta m}^{\sigma'}(E)$.

Evaluation of $S_{\alpha\beta}^{\sigma\sigma'}\equiv S_{\alpha\beta}^{\sigma\sigma'}(\omega=0,\ T=0)$ at zero-temperature (where Johnson-Nyquist thermal contribution vanishes and the Fermi function is a step function $f_\alpha^\rho(E)=\theta(E-\mu_\alpha^\rho)$) and zero-frequency in the top lead $\alpha=\beta=2$ of a four-terminal bridge typically employed in the analysis of the mesoscopic SHE [13,27] yields explicit expressions for $S_{22}^{\sigma\sigma'}$, $S_{22}^{\rm spin}$, and $S_{22}^{\rm charge}$ noise power (for labeling of the four leads see inset in the middle panel of fig. 1(a)). They are too lengthy to be written down explicitly due to numerous terms arising from the effect of other leads on the shot noise in selected lead 2. Using the unitarity of the scattering matrix, $S_{22}^{\sigma\sigma'}$ can be expressed solely in terms of the transmission matrix $\mathbf{t}_{\alpha\beta}^{\sigma\sigma'}$, which is a block of the full scattering matrix determining the probability $|[\mathbf{t}_{\alpha\beta}^{\sigma\sigma'}]_{nm}|^2$ for spin-σ' electron incident in lead β in the orbital conducting channel $|m\rangle$ to be transmitted to lead α as spin-σ electron in channel $|n\rangle$.

Since in two-terminal devices the spin interaction effects on the shot noise are most pronounced when the injected current is spin-polarized [20–22], we also compute noise correlators for setups where spin-polarized charge current is injected through lead 1 thereby driving the transverse charge Hall current [30] through leads 2 and 3. In this case, the magnitude $|\mathbf{P}|$ of the spin-polarization vector enters into eq. (7) via the spin-dependent electrochemical potentials in the injecting lead 1, $\mu_1^\uparrow=E_F+eV$ and $\mu_1^\downarrow=E_F+eV(1-|\mathbf{P}|)/(1+|\mathbf{P}|)$, where E_F is the Fermi energy of electrons in the macroscopic reservoirs. Such setup [30] is also closely related to the inverse SHE, where $\mu_1^\uparrow=E_F+eV=\mu_2^\downarrow$ and $\mu_1^\downarrow=E_F=\mu_2^\uparrow$ describes injection of two counterpropagating fully spin-polarized charge currents of opposite $\mathbf{P}$ and, therefore, no net longitudinal charge current [6].

In general, the central 2DEG sample employed in SHE experiments [2] can be modeled by the effective mass Hamiltonian which takes into account intrinsic and extrinsic SO coupling effects, as well as the impurity $V_{\rm dis}(x,y)$ and confining $V_{\rm conf}(y)$ potentials

$$\hat{H} = \frac{\hat{p}_x^2+\hat{p}_y^2}{2m^*}+V_{\rm conf}(y)+V_{\rm dis}(x,y) +\frac{\alpha}{\hbar}(\hat{p}_y\hat{\sigma}_x-\hat{p}_x\hat{\sigma}_y)+\lambda(\hat{\boldsymbol{\sigma}}\times\hat{\mathbf{p}})\cdot\nabla V_{\rm dis}(x,y). \quad (8)$$

Here the fourth term is the intrinsic Rashba SO coupling [31] due to structural inversion asymmetry of the quantum well ($(\hat{\sigma}_x,\hat{\sigma}_y,\hat{\sigma}_z)$ denotes the vector of the Pauli matrices, and $\hat{\mathbf{p}}=(\hat{p}_x,\hat{p}_y)$ is the momentum operator in 2D space), which is responsible for $\Delta_{\rm SO}=2\alpha k_F$ spin splitting at the Fermi level ($\hbar k_F$ is the Fermi momentum). The fifth term is a relativistic correction to the Pauli equation for spin-$\frac{1}{2}$ particle where the minuscule value of λ in vacuum can be renormalized enormously by the band structure effects due to strong crystal potential (leading to, *e.g.*, $\lambda/\hbar=5.3\,\text{Å}^2$ for GaAs [31]).

The consequences of eq. (7) can be explored by analytical means, such as the wave function matching [32] (for one or two channel leads attached to ballistic structures) or random matrix theory applicable to "black-box" disordered and chaotic ballistic structures [29]. However, to take into account concurrent microscopic modeling [15] of the impurity scattering, SO effects (skew-scattering and side jump [15,17]) in the electric field of an impurity, and fast spin precession induced by strong intrinsic SO coupling effects, it is more advantageous to employ the nonperturbative real⊗spin space Green functions [10,13]. For this purpose, we represent the general 2DEG Hamiltonian eq. (8) in the local orbital basis [26]

$$\hat{H}_{\rm TB} = \sum_{\mathbf{m},\sigma}\varepsilon_{\mathbf{m}}\hat{c}_{\mathbf{m}\sigma}^\dagger\hat{c}_{\mathbf{m}\sigma}+\sum_{\langle\mathbf{m}\mathbf{m}'\rangle}\sum_{\sigma\sigma'}\hat{c}_{\mathbf{m}\sigma}^\dagger t_{\mathbf{m}\mathbf{m}'}^{\sigma\sigma'}\hat{c}_{\mathbf{m}'\sigma'} -i\lambda_{\rm SO}\sum_{\mathbf{m},\alpha\beta}\sum_{ij}\sum_{\nu\gamma}\epsilon_{ijz}\nu\gamma(\varepsilon_{\mathbf{m}+\gamma\mathbf{e}_j}-\varepsilon_{\mathbf{m}+\nu\mathbf{e}_i}) \times\hat{c}_{\mathbf{m},\alpha}^\dagger\hat{\sigma}_{\alpha\beta}^z\hat{c}_{\mathbf{m}+\nu\mathbf{e}_i+\gamma\mathbf{e}_j,\beta}. \quad (9)$$

The first term accounts for isotropic short-range spin-independent static impurity potential where $\varepsilon_{\mathbf{m}}\in[-W/2,W/2]$ is a uniform random variable. The second term is the tight-binding representation of the Rashba SO coupling whose nearest-neighbor $\langle\mathbf{m}\mathbf{m}'\rangle$ hopping is a non-trivial 2×2 Hermitian matrix $t_{\mathbf{m}'\mathbf{m}}=(t_{\mathbf{m}\mathbf{m}'})^\dagger$ in the spin space

$$\mathbf{t}_{\mathbf{m}\mathbf{m}'} = \begin{cases} -t_{\rm O}\mathbf{I}_s - it_{\rm SO}\hat{\sigma}_y & (\mathbf{m}=\mathbf{m}'+\mathbf{e}_x), \\ -t_{\rm O}\mathbf{I}_s + it_{\rm SO}\hat{\sigma}_x & (\mathbf{m}=\mathbf{m}'+\mathbf{e}_y). \end{cases} \quad (10)$$

Here $\mathbf{I}_s$ is the unit 2×2 matrix in the spin space. The strength of the SO coupling is measured by the parameter $t_{\rm SO}=\alpha/2a$ (a is the lattice spacing), and the spin-splitting of the band structure is expressed as $\Delta_{\rm SO}=4at_{\rm SO}k_F$ in terms of $t_{\rm SO}$.

A direct correspondence between the continuous effective mass Hamiltonian eq. (8) and its lattice version eq. (9) is established by selecting the Fermi energy of the injected electrons to be close to the bottom of the band where tight-binding dispersion reduces to the parabolic one, and by using $t_{\rm O}=\hbar^2/(2m^*a^2)$ for the orbital hopping which yields the effective mass m^* in the continuum limit. The labels in the third term, which involves both nearest-neighbor and next-nearest-neighbor hopping, are: the dimensionless extrinsic SO scattering strength $\lambda_{\rm SO}=\lambda\hbar/(4a^2)$; ϵ_{ijz} stands for the Levi-Civita totally antisymmetric tensor with i, j denoting the in-plane coordinate axes; and ν, γ are the dummy indices taking values ± 1.

The computation [10,13] of $\mathbf{t}^{\sigma\sigma'}_{\alpha\beta}$ for multiterminal structures described by eq. (9) requires to find the retarded Green function of the scattering region $\hat{G}^r = [E-\hat{H}_{\rm open}]^{-1}$ associated with the Hamiltonian $\hat{H}_{\rm open}=\hat{H}_{\rm TB}+\sum_{\alpha,\sigma}\hat{\Sigma}^{r,\sigma}_\alpha$ of the open system. Here non-Hermitian retarded self-energy matrices $\hat{\Sigma}^{r,\sigma}_\alpha$ introduced by the interaction with the leads determine escape rates of spin-σ electrons into the electrodes. The block $\hat{G}^{r,\sigma\sigma'}_{\alpha\beta}$ of the retarded Green function matrix, consisting of those matrix elements which connect the layer of the sample attached to lead β to the layer of the sample attached to lead α, yields the spin-resolved transmission matrix

$$\mathbf{t}^{\sigma\sigma'}_{\alpha\beta} = 2\sqrt{-{\rm Im}\,\hat{\Sigma}^{r,\sigma}_\alpha}\cdot\hat{G}^{r,\sigma\sigma'}_{\alpha\beta}\cdot\sqrt{-{\rm Im}\,\hat{\Sigma}^{r,\sigma'}_\beta}. \qquad (11)$$

The spin quantization axis for $\uparrow$ and $\downarrow$ spin states is assumed to be the z-axis, so that all spin currents and noises in lead 2 and 3 describe the SHE response of a 2DEG.

The effective momentum-dependent magnetic field within the plane of 2DEG, corresponding to the Rashba SO coupling, causes injected z-polarized spins to precess, thereby breaking the conservation of S_z spin. This process is characterized by the spin precession length $L_{\rm SO}$, along which injected out-of-plane polarized spins precess by an angle π. The $L_{\rm SO}$ scale plays a crucial role in the mesoscopic SHE [13]. It is inversely proportional to the Rashba coupling strength, $L_{\rm SO}=\pi\hbar^2/2m^*\alpha$ (typically $L_{\rm SO}\sim 100\,{\rm nm}$), and can be extracted from the measurements of spin dephasing in both ballistic and diffusive systems. The numerically exact real$\otimes$spin space non-equilibrium Green function approach allows us to treat both weakly ($L \ll L_{\rm SO}$) and strongly ($L \geqslant L_{\rm SO}$) SO-coupled multichannel nanostructures, as well as their shape, arrangement of the attached electrodes, and disorder involved in the extrinsic SO coupling.

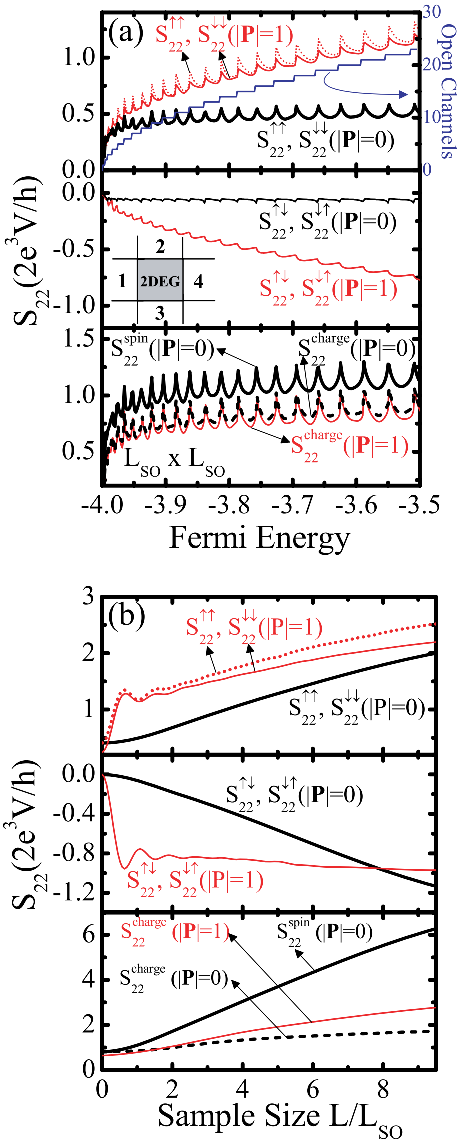

Fig. 1: (Color online) Ballistic spin-resolved shot noise in the transverse electrode 2 (see inset in panel (a)), as well as the total shot noise of pure spin Hall current (driven by unpolarized $|\mathbf{P}|=0$ injected charge current I_1) or charge Hall current (driven by spin-polarized $\mathbf{P}=(0,0,1)$ injected I_1), in *clean* 2DEGs with the Rashba SO coupling as a function of: (a) Fermi energy E_F; or (b) Rashba SO coupling α measured through the spin precession length $L_{\rm SO}=\pi\hbar^2/2m^*\alpha$. In panel (a) the 2DEG sample is of the size $L_{\rm SO}\times L_{\rm SO}$, while in panel (b) the sample size is $300\,{\rm nm}\times 300\,{\rm nm}$ and E_F is fixed to open 23 channels for electron injection from lead 1.

Multiterminal spin and charge shot noise in ballistic 2DEG nanostructures. – In this section and related fig. 1 we assume ballistic transport ($V_{\rm dis}(x,y)=0$ or $\varepsilon_{\mathbf{m}}=0$) through 2DEG with non-zero $L_{\rm SO}$ due to the Rashba coupling. We recall that in two-terminal ballistic structure the stream of electrons (injected from noiseless electrodes) is completely correlated by the Pauli principle in the absence of impurity backscattering, so that the corresponding shot noise vanishes, $S=0$ (except at the subband edges where new conducting channels open up) [19]. The non-zero noise $S=2FeI$ requires stochasticity of quantum-mechanical scattering off impurities or walls of chaotic cavities which, together with Pauli blocking or Coulomb interactions, determine the Fano factor F (such as the well-known $F=1/3$ in diffusive conductors or $F=1/4$ in chaotic ballistic cavities for transport of non-interacting electrons [19]). However, in four-terminal structures in fig. 1 transmission is not perfect because of the presence of the transverse leads (even if they do not draw current [33]), so that non-zero noise appears in the absence of SO coupling. While large Rashba coupling would introduce backscattering [13,27]

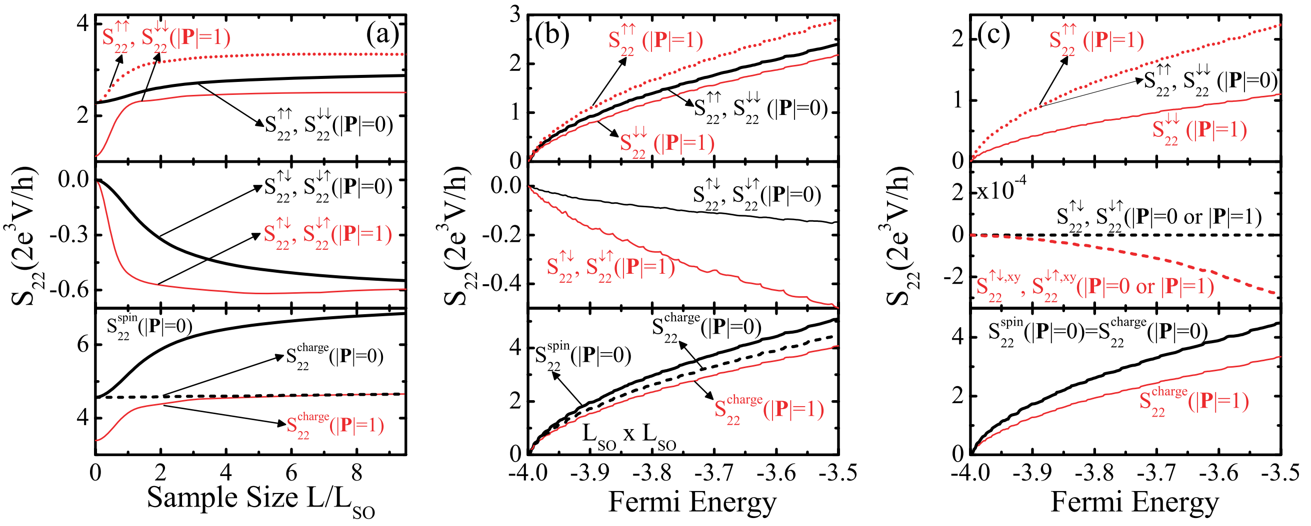

Fig. 2: (Color online) Diffusive spin-resolved shot noise in the transverse electrode 2, as well as the total shot noise of pure spin Hall current (for unpolarized $|\mathbf{P}|=0$ injection of I_1) or charge Hall current (for spin-polarized $\mathbf{P}=(0,0,1)$ injection of I_1), in *disordered* four-terminal 2DEGs with the Rashba SO coupling (panels (a) and (b)) or extrinsic SO scattering of strength $\lambda/\hbar = 5.3$ Å^2 (panel (c)). In panel (b) the 2DEG sample is of the size $L_{SO}\times L_{SO}$, while in panels (a), (c) the sample size is fixed at 300 nm × 300 nm. The Fermi energy in panel (a) is set to allow for 23 open conducting channels (see fig. 1(a)).

at the interface between the electrodes with no SO coupling and the sample, we find this effect not to be the crucial one for noise discussion below, since similar results are obtained for the bridge where leads 1 and 4 have the same Rashba SO coupling as in the central 2DEG sample.

Since the magnitude of the mesoscopic SHE increases with the sample size L, reaching optimal value [13,34] when $L\simeq L_{SO}$, we employ the 2DEG sample of size $L_{SO}\times L_{SO}$ to study the dependence of the shot noise on the Fermi energy (*i.e.*, charge density). We also assume that 2DEG is smaller than the inelastic scattering length L_{in} because in larger samples electron-phonon scattering averages out the shot noise to zero [35]. The most conspicuous feature of spin-resolved noise in fig. 1 is the emergence of highly non-trivial cross-correlations between spin-resolved currents encoded by $S_{22}^{\uparrow\downarrow}=S_{22}^{\downarrow\uparrow}<0$ (more pronounced for polarized $\mathbf{P}=(0,0,1)$ injection). This stems from spin-flips in the form of continuous spin precession of the z-axis–oriented spins in the effective momentum-dependent magnetic field of the Rashba SO coupling [22]. Such cross-correlations can be manipulated by changing the Fermi energy in the case of polarized injection ($|\mathbf{P}|=1$) or Rashba coupling in the case of unpolarized longitudinal current ($\mathbf{P}=0$), thereby imprinting signatures of the intrinsic SO coupling on experimentally measurable charge current noise S_{22}^{charge}.

Another feature specific to mesoscopic manifestations of SHE, which is also exhibited by the SHE conductance $I_2^{S_z}/V$ [13,27], is the appearance of sharp noise peaks in fig. 1(a) in the vicinity of subband edges. At these energies new conducting channels in the leads become available for transport (top panel of fig. 1(a)). Although this multiterminal noise property of ballistic conductors persists even in the absence of SO coupling, additional features of this type can arise at the energies of bound states in the cross device geometry whose mixing with propagating states via SO coupling introduces resonances in the transmission [30].

We emphasize [13,26] that achieving pure ($I_2=I_3=0$) spin Hall current $I_2^{S_z}$, akin to SHE in infinite systems [9,14], requires to apply [13,25] voltages $\mu_2=\mu_3=eV/2$ to transverse leads of the clean bridge biased with $\mu_1=eV$ and $\mu_4=0$. Despite zero charge current $I_2=0$ in this case, we find non-zero fluctuations around zero average value as measured by $S_{22}^{\text{charge}}(|\mathbf{P}|=1)$ in fig. 1. The noise power increases in the same setup, at fixed E_F and with fast spin dynamics in samples $L/L_{SO}\gtrsim 2$, by switching from unpolarized to polarized injection of longitudinal current I_1 responsible for non-zero transverse charge Hall current [30]. Note that due to $I_2=0$ in the SHE setup ($|\mathbf{P}|=0$), we plot raw noise values in all figures rather than normalizing them to $2eI_2$ or $2eI_1$ (to get the usual Fano factors).

Multiterminal spin and charge shot noise in diffusive 2DEG nanostructures. – To bring a multiterminal SHE bridge into the diffusive transport regime, we introduce disorder into the 2DEG through the on-site potential $\varepsilon_{\mathbf{m}}\in[-W/2,W/2]$ in Hamiltonian eq. (9) and tune its strength $W=1.1t_O$ to *ensure* that the shot noise in lead 1 attains the universal value $F_{11}=S_{11}^{\text{charge}}/2eI_1=1/3$ characterizing diffusion in multiterminal devices [33]. In the absence of the SO coupling, the noise in the other three leads does not display any universal features ($F_{11}=1/3$ is expected to be independent of the impurity distribution, band structure, and shape of the conductor [33]) because of non-local effects —that is, other leads contribute to the noise in an electrode $\alpha \neq 1$ making possible arbitrarily large values of $F_{\alpha\alpha}$ [33].

In the presence of disorder, one can expect both extrinsic and intrinsic contributions to $I_2^{S_z}$. Their importance (as in the case of experimentally explored SHE systems based on 2DEGs [2]) is governed [26] by the ratio of the characteristic energy scales $\Delta_{\rm SO}\tau/\hbar$, where $\hbar/\tau$ is the disorder-induced broadening of energy levels due to transport scattering time τ. For simplicity, we analyze separately 2DEGs with dominant intrinsic ($\alpha \neq 0$, $\lambda = 0$ in fig. 2(a),(b)) and extrinsic ($\alpha = 0$, $\lambda/\hbar = 5.3\,\text{Å}^2$ in fig. 2(c)) regimes of SHE. The most important insight brought about by fig. 2 is the substantial difference between the shot noise in the intrinsic (fig. 2(a),(b)) and extrinsic (fig. 2(c)) regimes, where the former exhibits non-zero cross-correlations $S_{22}^{\uparrow\downarrow} = S_{22}^{\downarrow\uparrow} < 0$ akin to its ballistic counterpart in fig. 1 but smaller. The shot noise of the extrinsic SHE device in fig. 2(c) has no correlations of this type for the z-axis spins, while exhibiting orders of magnitude smaller cross-correlation noise, $S_{22}^{\uparrow\downarrow,x}$ and $S_{22}^{\uparrow\downarrow,y}$ for the x- or y-spins, respectively, which carry no spin current $I_2^{S_x} = I_2^{S_y} \equiv 0$, when $\lambda \neq 0$. We also find that hypothetical (*i.e.*, experimentally not accessible) increase of λ would give orders of magnitude smaller noise change (in fact, decrease) compared to significant spin $S_{22}^{\rm spin}(|\mathbf{P}| = 0)$ or charge $S_{22}^{\rm charge}(|\mathbf{P}| = 1)$ shot noise enhancement with increasing of the intrinsic α that can be experimentally controlled [36].

Conclusions. – We predict that in low-dimensional mesoscopic SHE systems any intrinsic SO mechanisms involving *precessing spins* would lead to significant enhancement of the shot noise of spin and charge transport, as well as to non-trivial correlations between spin-resolved currents of opposite spin states in the transverse electrodes. In sharp contrast, the extrinsic SO scattering off impurities in 2D has no measurable effect on the shot noise. Therefore, experiments observing shot noise enhancement in the transverse electrodes upon changing the voltage of the gate electrode [36] covering 2DEG could unambiguously resolve the dominance of the intrinsic contribution to the spin Hall or the charge Hall effect (and related inverse SHE) in multiterminal nanostructures.

* * *

Financial support from DOE Grant No. DE-FG02-07ER46374 and NSF Grant No. ECCS 0725566 is gratefully acknowledged.

REFERENCES

[1] Kato Y. K. *et al.*, *Science*, **306** (2004) 1910.

[2] Sih V. *et al.*, *Nat. Phys.*, **1** (2005) 31.

[3] Valenzuela S. O. and Tinkham M., *Nature*, **442** (2006) 176; Saitoh E. *et al.*, *Appl. Phys. Lett.*, **88** (2006) 182509; Kimura T. *et al.*, *Phys. Rev. Lett.*, **98** (2007) 156601.

[4] Awschalom D. D. and Flatté M. E., *Nat. Phys.*, **3** (2007) 153.

[5] Hirsch J. E., *Phys. Rev. Lett.*, **83** (1999) 1834.

[6] Hankiewicz E. M. *et al.*, *Phys. Rev. B*, **72** (2005) 155305.

[7] Nagaosa N., *J. Phys. Soc. Jpn.*, **77** (2008) 031010.

[8] Murakami S., Nagaosa N. and Zhang S.-C., *Science*, **301** (2003) 1348.

[9] Sinova J. *et al.*, *Phys. Rev. Lett.*, **92** (2004) 126603.

[10] Nikolić B. K., Zârbo L. P. and Souma S., *Phys. Rev. B*, **73** (2006) 075303.

[11] Nikolić B. K. *et al.*, *Phys. Rev. Lett.*, **95** (2005) 046601.

[12] Zyuzin V. A., Silvestrov P. G. and Mishchenko E. G., *Phys. Rev. Lett.*, **99** (2007) 106601.

[13] Nikolić B. K., Zârbo L. P. and Souma S., *Phys. Rev. B*, **72** (2005) 075361.

[14] Guo G. Y. *et al.*, *Phys. Rev. Lett.*, **100** (2008) 096401.

[15] Hankiewicz E. M. and Vignale G., *Phys. Rev. Lett.*, **100** (2008) 026602.

[16] Souma S. and Nikolić B. K., *Phys. Rev. Lett.*, **94** (2005) 106602.

[17] Sinitsyn N. A., *J. Phys.: Condens. Matter*, **20** (2008) 023201.

[18] Kötzler J. and Gil W., *Phys. Rev. B*, **72** (2005) 060412(R).

[19] Blanter Y. M. and Büttiker M., *Phys. Rep.*, **336** (2000) 1.

[20] Mishchenko E. G., *Phys. Rev. B*, **68** (2003) 100409(R); Lamacraft A., *Phys. Rev. B*, **69** (2004) 081301(R); Belzig W. and Zareyan M., *Phys. Rev. B*, **69** (2004) 140407(R); Nagaev K. E. and Glazman L. I., *Phys. Rev. B*, **73** (2006) 054423.

[21] Hatami M. and Zareyan M., *Phys. Rev. B*, **73** (2006) 172409.

[22] Dragomirova R. L. and Nikolić B. K., *Phys. Rev. B*, **75** (2007) 085328.

[23] Guerrero R. *et al.*, *Phys. Rev. Lett.*, **97** (2006) 266602; Garzon S., Chen Y. and Webb R., *Physica E*, **40** (2007) 133.

[24] Timm C., von Oppen F. and Höfling F., *Phys. Rev. B*, **69** (2004) 115202.

[25] Erlingsson S. I. and Loss D., *Phys. Rev. B*, **72** (2005) 121310(R).

[26] Nikolić B. K. and Zârbo L. P., *EPL*, **77** (2007) 47004.

[27] Sheng L. and Ting C. S., *Int. J. Mod. Phys. B*, **20** (2006) 2339.

[28] Hankiewicz E. M. *et al.*, *Phys. Rev. B*, **70** (2004) 241301.

[29] Bardarson J. H., Adagideli I. and Jacquod Ph., *Phys. Rev. Lett.*, **98** (2008) 196601.

[30] Bulgakov E. N. *et al.*, *Phys. Rev. Lett.*, **83** (1999) 376.

[31] Winkler R., *Spin-Orbit Coupling Effects in Two-Dimensional Electron and Hole Systems* (Springer, Berlin) 2003.

[32] Egues J. C., Burkard G. and Loss D., *Phys. Rev. Lett.*, **89** (2002) 176401.

[33] Sukhorukov E. V. and Loss D., *Phys. Rev. B*, **59** (1999) 13054.

[34] Moca C. P. and Marinescu D. C., *Phys. Rev. B*, **75** (2007) 035325.

[35] Steinbach A. H., Martinis J. M. and Devoret M. H., *Phys. Rev. Lett.*, **76** (1996) 3806.

[36] Nitta J. *et al.*, *Phys. Rev. Lett.*, **78** (1997) 1335; Grundler D., *Phys. Rev. Lett.*, **84** (2000) 6074.